



Precise Measurement of Muon Capture on the Proton^{*}

P. KAMMEL¹, V. A. ANDREEV², D. V. BALIN², R. M. CAREY³, T. CASE⁴,
D. B. CHITWOOD¹, S. M. CLAYTON¹, K. M. CROWE⁴, J. DEUTSCH⁵,
P. T. DEBEVEC¹, P. U. DICK⁶, A. DIJKSMAN⁶, J. EGGER⁶, D. FAHRNI⁶,
A. A. FETISOV², S. J. FREEDMAN⁴, V. A. GANZHA², B. GARTNER⁴,
J. GOVAERTS⁵, F. E. GRAY¹, F. J. HARTMANN⁷, W. D. HEROLD⁶,
D. W. HERTZOG¹, V. I. JATSOURA², A. G. KRIVSHICH², B. LAUSS⁴,
E. M. MAEV², O. E. MAEV², V. E. MARKUSHIN⁶,
C. J. G. ONDERWATER¹, C. PETITJEAN⁶, G. E. PETROV², C. C. POLLY¹,
R. PRIEELS⁵, S. M. SADETSKY², G. N. SCHAPKIN², R. SCHMIDT⁶,
G. G. SEMENCHUK², M. SOROKA², A. A. VOROBYOV² and
N. I. VOROPAEV²

¹University of Illinois at Urbana-Champaign, Urbana, IL 61801, USA

²Petersburg Nuclear Physics Institute (PNPI), Gatchina 188350, Russia

³Boston University, Boston, MA 02215, USA

⁴University of California Berkeley, UCB and LBNL, Berkeley, CA 94720, USA

⁵Université Catholique de Louvain, B-1348 Louvain-La-Neuve, Belgium

⁶Paul Scherrer Institute, CH-5232 Villigen, Switzerland

⁷Technische Universität München, D-85747 Garching, Germany

Abstract. The aim of the μ Cap experiment is a 1% measurement of the singlet capture rate Λ_S for the basic electro-weak reaction $\mu + p \rightarrow n + \nu_\mu$. This observable is sensitive to the weak form-factors of the nucleon, in particular to the induced pseudoscalar coupling constant g_p . It will provide a rigorous test of theoretical predictions based on the Standard Model and effective theories of QCD. The present method is based on high precision lifetime measurements of μ^- in hydrogen gas and the comparison with the free μ^+ lifetime. The μ^- experiment will be performed in ultra-clean, deuterium-depleted H_2 gas at 10 bar. Low density compared to liquid H_2 is chosen to avoid uncertainties due to $pp\mu$ formation. A time projection chamber acts as a pure hydrogen active target. It defines the muon stop position in 3D and detects rare background reactions. Decay electrons are tracked in cylindrical wire-chambers and a scintillator array covering 75% of 4π .

Key words: muon, capture, proton, pseudoscalar form factor, TPC.

1. Introduction

The goal of this experiment [1–3] is a determination of the rate Λ_S of the basic charged-current reaction



^{*} Work supported by Paul Scherrer Institute, Russian Ministry of Science and Technology, US Department of Energy, US National Science Foundation and INTAS.

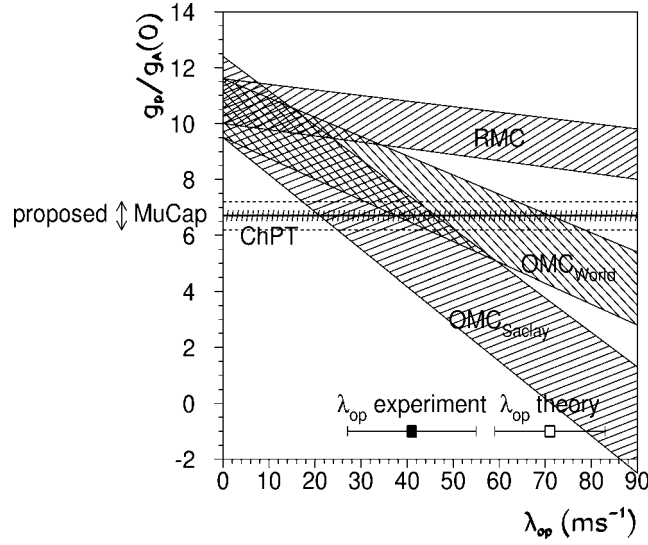


Figure 1. Current constraints on g_p as function of the ortho–para transition rate λ_{OP} (c.f. [5]). Experimental results from ordinary muon capture (OMC) [6], radiative muon capture (RMC) [5], and chiral perturbation theory (ChPT).

via the lifetime of μ^- bound in the singlet $p\mu^-$ ($F = 0$) system to an accuracy $\delta\tau_\mu/\tau_\mu$ better than 10^{-5} . The comparison of $\tau_\mu = 1/\lambda_\mu$ for $p\mu$ atoms with that for free μ^+ 's will considerably improve the determination of the induced pseudoscalar coupling constant g_p ($q_0^2 = -0.88m_\mu^2$) to the level $\delta g_p/g_p \leq 7\%$. The μ^+ lifetime will be measured simultaneously as a reference and to check systematics. The lifetime measurements will be done with a time projection chamber (TPC) filled with 10 bar of ultra-pure deuterium-depleted hydrogen surrounded by multi-wire proportional chambers and a hodoscope of scintillation detectors.

Precision measurements of muon capture by the proton provide a challenging opportunity to test our understanding of chiral symmetry breaking in QCD. In the absence of second class currents, the electroweak structure of the nucleon can be described by four form factors g_V , g_M , g_A , and g_p that determine the matrix elements of the charged vector and axial currents. While the first three of these form factors are well determined by Standard Model symmetries and experimental data, the pseudoscalar form factor g_p is experimentally known to much less precision (Figure 1). The recent RMC result $g_p = 12.2 \pm 0.9 \pm 0.4$ [5] exceeds the theoretical predictions by 4.2σ . The precision of the older OMC results was mainly limited by absolute calibration of the neutron detectors. The most accurate measurement with 4.5% precision was performed in Saclay [6] using the lifetime technique in a liquid hydrogen target. At this high density $p\mu$ capture proceeds not only from the free proton, but also from the ortho and para states of the $pp\mu$ molecule. The uncertainty in the transition rate λ_{op} between these states leads to a significant error in the interpretation of this measurement. A recent experiment on $\mu^3\text{He}$ capture [7]

Table I.

	Reference				
	[8]	[14]	[13]	[11]	[12]
g_P	8.44 ± 0.23	8.21 ± 0.09	8.475 ± 0.076		
Λ_S (s^{-1})			688.4 ± 3.8	695	687.4
Λ_T (s^{-1})			12.01 ± 0.12	11.9	12.9

gives $g_P = 8.53 \pm 1.54$ (the accuracy is limited by the theoretical extraction of g_P from the three-nucleon system) in better agreement with theory.

This controversial experimental situation is in stark contrast to the recent progress in the theoretical understanding of muon capture achieved within the framework of low energy effective theories of QCD. The dominant contribution to the pseudoscalar form factor is given by the pion pole (PCAC), and the leading correction to the pole term can be derived from QCD Ward identities [8] confirming the old current-algebra result [9]. Possible higher order corrections appear to be small [10]. Recent calculations of singlet and triplet muon capture rates in heavy-baryon chiral perturbation theory [11] and in the small-scale expansion [12] are in a good agreement with the careful analysis [13].

The main experimental challenges for a significantly improved measurement of Λ_S result from three different sources.

- (a) Statistics: The capture rate will be determined as $\Lambda_S = \lambda_{\mu^-} - \lambda_{\mu^+}$, thus $\delta\Lambda_S \sim \sqrt{2}\delta\lambda_{\mu}$. As $\Lambda_S \approx 1.5 \times 10^{-3}\lambda_{\mu}$ the lifetime of the positive and negative muon have to be measured with at least 10 ppm precision, i.e., 10^{10} reconstructed events each.
- (b) Interpretation: $pp\mu$ formation should be slow so that capture takes place predominantly from the well defined $F = 0$ hfs states of the muonic hydrogen atom.
- (c) Distortions of the muon decay time spectrum: Dangerous physics effects for μ^- include direct or delayed muon stops in the wall material, transfer to gas impurities or to deuterium. The μ^+ polarization is partially preserved in hydrogen, leading to effects of muon spin rotation and relaxation. Detector imperfections might cause time dependent efficiency variations due to instrumental correlations between a muon and its decay electron and overlapping muon–electron pairs.

2. Experimental set-up

The central part of our detector is a time projection chamber (TPC) embedded in a pressure vessel filled with 10 bar of ultra-pure deuterium-depleted hydrogen (protium). The TPC which was specially developed for this experiment has a sensitive volume of $15 \times 12 \times 30$ cm³ and acts as active target monitoring all muon stops and

electrons from muon decay. The vertical drift field of ~ 2.4 kV/cm causes electrons to drift with a velocity of ~ 0.7 cm/ μ s toward multiwire proportional planes at the bottom. There, charges are amplified by typically a factor of 10^4 and read out by 75 anode wires in x -direction and by 38 cathode strips made of wires in z -direction. The y -coordinate, defining the height in the TPC, is determined by the drift time which ranges from 0 to 17 μ s. Incoming muons are detected by two planes of wire chambers in front of the TPC. Track reconstruction inside the TPC clearly distinguishes between muons stopping in H_2 versus in the walls, thus allowing the use of low gas density (1% of liquid H_2) which reduces problem (b) to a negligible level.

The pressure chamber has cylindrical walls made of 4 mm aluminum to reduce multiple scattering of through-going decay electrons. The hydrogen vessel and its interior wire chambers are made of clean materials (metals, ceramics, quartz-glass frames, etc.) that can be baked out up to 150°C and evacuated down to 10^{-7} – 10^{-8} mbar. This level is required to maintain a required hydrogen purity of 10^{-8} . Ultra clean protium is filled via a specially developed gas system using chemical purifying methods. The gas can be circulated and purified during the measurements. Since this is an active target experiment, very low levels of impurities can be determined from the chamber signals themselves, in addition to chromatographic gas analysis.

Surrounding the pressure tank, two cylindrical proportional chambers and an array of plastic detectors are mounted covering an effective solid angle $\Omega/4\pi \sim 75\%$. For the electron time determination, the measurements will rely entirely on the detectors outside the hydrogen pressure vessel, i.e., on the two wire chambers for directional back tracking and on the plastic hodoscope for the absolute time measurement. The separation of detector functions for electrons from those for muons ensures independent absolute time measurements without the danger of electronic cross-talks and tail effects. The tracking chambers can handle event rates of ~ 30 kHz, since pile-up problems can be reduced by identifying the muon–electron pair originating from a common vertex. This method also suppresses other possible background.

A coil will be installed outside the TPC vessel to generate a uniform magnetic field of ~ 70 Gauss transverse to the beam and muon spin axis. This field will precess the remaining free muon polarization at 1 MHz creating a sinusoid on top of the exponential decay spectrum. Monte Carlo studies indicate that amount and relaxation of this polarization can be determined in a fit over 15 μ s. The oscillating part largely decouples from the lifetime measurement. Moreover spin asymmetries get strongly reduced by the cylindrical symmetry of the setup.

3. Detector performance

Significant R&D was required to establish the feasibility of the new method and to optimize physics and detector parameters. In particular, several engineering runs with a prototype TPC have been performed at PSI (cf. contribution [4] and ref-

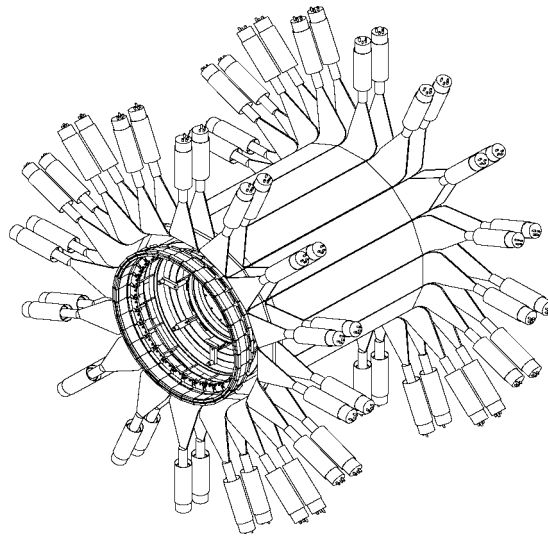


Figure 2. Overview of μ Cap detector showing scintillator array and endframes of the cylindrical wire chambers used for electron tracking. The hydrogen vessel with muon chambers and TPC is located inside the electron detector system.

erences [1–3]). The performance of the prototype detector was satisfactory and proved that stable chamber operation in pure hydrogen can be achieved. Rather high chamber voltages of 6.8 kV on 2–4 mm spacing were required in order to obtain sufficient gas amplification. The main data was recorded by a custom-designed dead-time free TDC (TDC400) operating at a clock rate of 5 MHz. The hits of all detectors were stored for contiguous time regions of ~ 10 ms, providing the full history information around individual muon stops. A short time slice from this time region is displayed in Figure 3.

The behavior of the observed μ^- decay rate is consistent with the decline of the target purity with time and purity recovery by refilling. The μ^+ spectra reveal μ^+ SR effects consistent with muonium precession in a residual magnetic field of 0.2–0.4 G (no transverse field was applied during this test). For pile-up free events the accidental to signal level is already $\sim 10^{-4}$ for a simple coincidence between a MWPC and electron telescope. It can be further improved by an order of magnitude using the 4 MWPC's and the TPC to precisely track the decay electron back to the end of the muon track (Figure 4).

By using the TPC as active target, charged products of muon induced reactions with impurities can be detected. Most critical are O_2 , N_2 , H_2O and D_2 . The TPC is sensitive to recoil nuclei (200–350 keV) from μ -capture on impurities with $Z > 1$ and from the $pd\mu$ fusion channel ${}^3\text{He}$ (0.2 MeV) + μ (5.3 MeV). The information is collected both with the TDC system and from 12 TPC anodes instrumented with FADC's. For the selection of μ -capture reactions logarithmic amplifiers, discriminators with high threshold about 70 keV and a hardware trigger were developed [4].

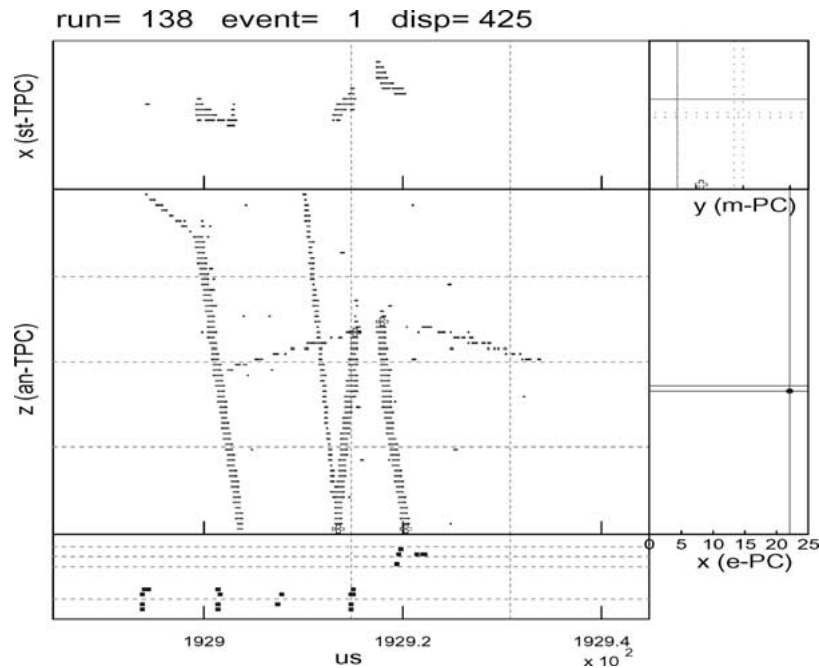


Figure 3. Event display of 60 μs time slice. The central panel (y - z plane) shows TPC anode signals as function of time (μs). Muons are distinguished from electrons by using two discriminator levels. The upper panel (y - x plane) indicates the corresponding information from the strip cathodes. The bottom panel shows the absolute times of various detector hits. The right panels indicate wires hits on muon (upper) and electron (lower) MWPC's, respectively.

For about 10^6 muon stops in the sensitive TPC volume 3876 μ -capture events with μ^- beam and only one event under the same requirements with μ^+ beam were found. As this data corresponds to an impurity level of 30 ppm as estimated by chemical analysis, a sensitivity to determine impurities with $Z > 1$ of about 0.01 ppm has been demonstrated.

Due to the ‘‘Ramsauer–Townsend’’ minimum in elastic $d\mu$ - p scattering, $d\mu$ atoms formed after transfer from protium can travel several cm in 10 bar hydrogen. Some fractions even leave the sensitive volume of the chamber, especially at late times after muon stop. Therefore, the μ - e time distribution can get significantly distorted toward a steeper slope simulating a larger capture rate. This is the principal reason why it is necessary to use protium which is strongly depleted from any deuterium. The distortions depend on the geometrical μ - e vertex cuts used, increasing with tighter cuts. Fortunately the diffusion correction can be self calibrated by monitoring deuterium impurities in the experiment and then extrapolating to zero deuterium concentration. The most promising method is the direct observation of muon diffusion by observing an electron track displaced from the muon stop point in the TPC. Figure 5 shows the result of a $d\mu$ diffusion search in our test runs. The outlying points in the left image are from the diffused $d\mu$ atoms

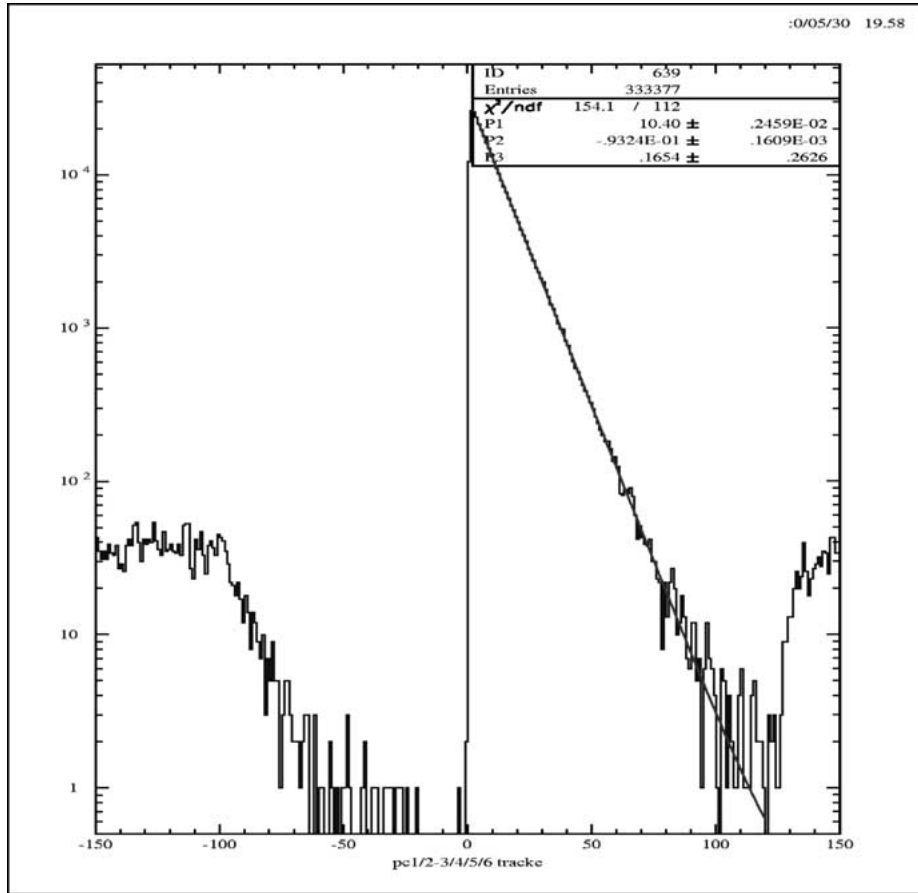


Figure 4. Time distribution of fully tracked μ - e events with global pile-up protection. The accidental level is below 10^{-5} of the signal at time 0.

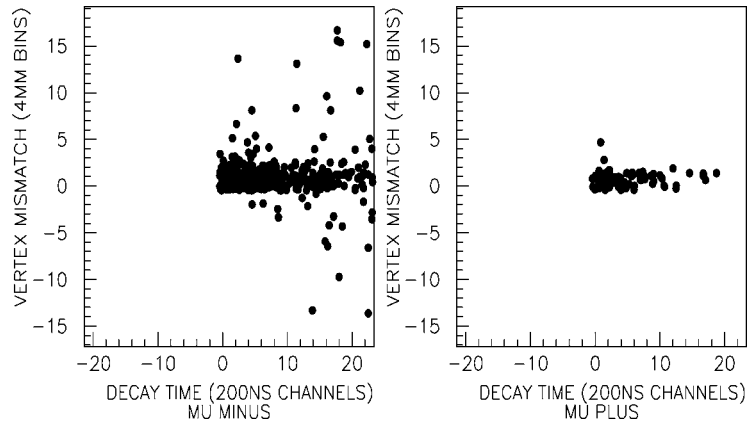


Figure 5. Distance between muon stop and decay point as function of decay time from μ - e tracks reconstructed inside the TPC. μ^- data (left), μ^+ data (right). Significant diffusion was observed for μ^- after $d\mu$ formation.

in a μ^- run. For reference only a single event at $t = 0$ leaks through in a μ^+ run shown on the right. Note the importance of the intrinsic TPC tracking accuracy and electron efficiency for this analysis.

4. Summary and outlook

We plan to analyze the data with two main and complementary methods.

Global pile-up free data. Only events are analyzed which do not have another muon entering the TPC within 10–20 μ s. This analysis is particularly clean and simple, and thus ideally suited for a precision experiment. Moreover it allows loose vertex cuts, thereby reducing the experimental sensitivity to deuterium diffusion. It has the disadvantage of significant pile-up losses.

Local pile-up free data. The TPC volume is subdivided in smaller volumes during the analysis by requiring no other local muon stop inside a cut volume around the electron reconstructed vector. In this way events can be analyzed where several simultaneous muons stop during the measurement/drift-time interval of the TPC. The vertex matching suppresses the accidental background from uncorrelated muons, but systematic corrections become more important.

The choice between the two analysis methods is made off-line, as in our experiment contiguous event-blocks containing all information are recorded. A summary of estimated statistical and systematic corrections and errors (indicated by parentheses) in ppm of the measured lifetimes is given in Table II.

The final μ Cap detector is presently under construction and first production running is expected in fall 2002. There exist several exciting future extensions of the physics reach for this program. A second phase of the experiment might aim at a 0.3% measurement of Λ_S to achieve an experimental precision of 3%

Table II.

	Global PU free data			Local PU free data		
	μ^-	μ^+	comment	μ^-	μ^+	comment
statistics	(10)	(10)	10^{10} events	(7)	(7)	2×10^{10} events
wall stops	(2)	–		(2)	–	
impurities	2(3)	–	for $c_Z = 10^{-8}$	2(3)	–	for $c_Z = 10^{-8}$
flat acc.	(2)	(2)	level 10^{-4}	(3)	(3)	level 5×10^{-4}
μ SR	–	(2)		–	(2)	
diffusion	1(1)	–	no vertex cut	100(5)	–	5 cm radial cut
two event corr.	–	–		(2)	(2)	acc. structure
total sys. error	4.2	2.8		7.1	4.1	
$\delta\lambda$ total error	10.9	10.4		10.	8.1	

in g_P matching the present theoretical error. This proposal is based on an intense chopped muon beam [15], which is presently being developed for the μLan experiment [16]. A very recent idea [17] concerns a precision measurement of the $d\mu$ capture process, both its integral rate and Dalitz Plot distribution. Within the framework of pion-less effective theories muon capture on the deuteron is directly related to the pp fusion in the sun [18] and neutrino deuteron scattering as observed in the Sudbury Neutrino Observatory [19] and, thus, appears a unique possibility to calibrate these fundamental processes of current topical interest.

Finally, let me express my sincere gratitude to Ken Nagamine and the organizers of MCF'01 for the opportunity to enjoy this stimulating meeting and let me congratulate him for his remarkable contributions to this field of muon physics.

References

1. Balin D. V. *et al.*, PSI proposal R-97-05 (1996) and documentation on <http://www.npl.uiuc.edu/exp/mucapture>.
2. Kammel P. *et al.*, *Nucl. Phys. A* **663/664** (2000), 911c; Kammel P., *AIP Conf. Proc.* **435** (1998), 419.
3. Vorobyov A. A. *et al.*, *Hyp. Interact.* **119** (1999), 13.
4. Maev E. M. *et al.*, *Hyp. Interact.*, this issue.
5. Wright D. H. *et al.*, *Phys. Rev. C* **57** (1998), 373.
6. Bardin G. *et al.*, *Phys. Lett. B* **104** (1981), 320.
7. Ackerbauer P. *et al.*, *Phys. Lett. B* **417** (1998), 224.
8. Bernard V., Kaiser N. and Meissner U. G., *Phys. Rev. D* **50** (1994), 6899.
9. Adler S. L. and Dothan Y., *Phys. Rev.* **151** (1966), 1267; Wolfenstein L., In: *High-Energy Physics and Nuclear Structure*, Plenum, NY, 1970, p. 661.
10. Bernard V., Hemmert T. R. and Meissner U., hep-ph/9811336, 1998.
11. Ando S., Myrer F. and Kubodera K., *Phys. Rev. C* **63** (2001), 015203.
12. Bernard V., Hemmert T. R. and Meissner U. G., *Nucl. Phys. A* **686** (2001), 290.
13. Govaerts J. and Lucio-Martinez J.-L., *Nucl. Phys. A* **678** (2000), 110.
14. Fearing H. W. *et al.*, *Phys. Rev. D* **56** (1997), 1783.
15. Kammel P. *et al.*, *Hyp. Interact.* **119** (1999), 323.
16. Carey R. *et al.*, <http://www.npl.uiuc.edu/exp/mulan>.
17. Kammel P. and Chen W. J., work in progress.
18. Butler M. and Chen J., *Phys. Lett. B* **520** (2001), 87, and reference given therein.
19. Ahmad Q. R. *et al.* [SNO Collaboration], *Phys. Rev. Lett.* **87** (2001), 071301.